Device simulation and optimization of HTL-free perovskite solar cell with $CH_3NH_3SnBr_3$ as the absorber layer using solar cell capacitance simulator software

M. V. Kavitha[a,b,*], C. K. Anjali[a], K. S. Sudheer[b]
[a]*Department of Physics ,Sree Narayana College, Nattika,University of Calicut, Kerala, India,PIN-680566*
[b]*Opto electronic Device simulation Research Lab, Department of Physics, Christ College (Autonomous), Irinjalakuda, University of Calicut, Kerala, India, PIN-680125*

Perovskite solar cells without a hole transport layer have gained popularity due to their stability and affordable manufacturing cost. In this work, device simulation of the solar cell structure is done using SCAPS-1D software with TiO_2 as the Electron Transport Layer while toxic-free compound $CH_3NH_3SnBr_3$ as the absorber material. The efficiency of the structure is found to be 12.63%. The cell performance parameters are investigated by varying individual cell parameters such as absorber layer thickness, absorber layer defect density and doping concentration, ETL thickness, ETL doping concentration, temperature and defect density of the absorber/ETL interface while holding others constant. Simulation with the optimised cell parameter values improves the efficiency to 24.02%.

(Received January 26, 2024; Accepted April 11, 2024)

Keywords: Simulation, Perovskite solar cells, HTL-free, Optimization

1. Introduction

Organo metal halide perovskites rapidly revolutionised the development of photo voltaic technology[1]. These materials have remarkable optoelectrical properties, such as tuneable bandgaps, high absorption coefficient, long carrier diffusion lengths and high charge carrier mobilities[2]. Lead-based perovskite technology represented a significant advance for the third generation[3,4]. Even though the efficiency of lead-based perovskites increased drastically in the last few years, their excessive toxicity and lack of long-term stability pose a threat to both the environment and human health [5,6,7]. For these reasons, we began using materials based on tin, including $CH_3NH_3SnX_3$, as the absorber. Features of tin-based perovskite include earth abundance, a high absorption coefficient, a suitable band gap, non-toxic behaviour, and a longer charge carrier life span[8,9,10].

HTL and ETL are the components of the planar structure (p-i-n and n-i-p) of perovskite solar cells, which aid in the collection and transportation of the holes and electrons generated, in their respective electrodes [11]. The HTL-free solar device is a new concept in the PV world which reduces the interface defect and fabrication cost without affecting the cell performance[1]. Hao, Liangsheng, et al [12] attained an efficiency of 20.45% for HTL-free FTO/ $CH_3NH_3SnI_3/C_{60}$/Au inverted structure in their simulation work. Sunny, Adil, et al. [1] modelled HTL-free PSC with the structure of FTO/TiO_2/$CH_3NH_3SnI_3$/Ni/glass and obtained an efficiency of 26.33%. Even though $CH_3NH_3SnI_3$ is a promising solar cell material from the band gap point of view, the optical properties of $CH_3NH_3SnBr_3$ make it a better absorber material[13]. Samiul Islam, Md, et al [14] modelled $TiO_2/CH_3NH_3SnBr_3$/NiO structure with HTL and obtained an efficiency of 21.66%.

In this work, device simulation of the HTL- Free perovskite solar cell structure is done using SCAPS-1D software with TiO_2 as the Electron Transport Layer while toxic-free compound $CH_3NH_3SnBr_3$ as the absorber material. With the initial simulation parameters obtained from

* Corresponding author: kavithajayajith@gmail.com
https://doi.org/10.15251/JOR.2024.202.245

published literature,the efficiency of the structure is found to be 12.63%. The cell performance parameters are investigated by varying individual cell parameters such as absorber layer thickness, absorber layer defect density and doping concentration, ETL thickness, ETL doping concentration, temperature, and interface defect density of the absorber/ETL interface while holding others constant. The simulation is repeated with optimised cell parameters.

2. Materials and methods

The structure of the HTL-free perovskite solar cell under study is FTO/TiO_2/$CH_3NH_3SnBr_3$/AU (Back Contact) and the schematic diagram is shown in Fig. 1. The initial simulation parameters of each layer and defect parameters obtained from published literature[14,15] are listed in Table 1 and Table 2 respectively. The simulations are done by one dimensional simulation program SCAPS-1D. This is based on solving Poisson's equation and continuity equations[16]. Simulations are done under the illumination of AM1.5G with an intensity of 1000W/m^2 at an operating temperature of 300K. The thermal velocities of holes and electrons are taken as 10^7cm/s. With the initial simulation parameters, the structure is simulated and the obtained performance parameters are listed in Table 3.The Current density -voltage curve and Quantum efficiency-wavelength curve are depicted in Fig.2 and Fig. 3 respectively.

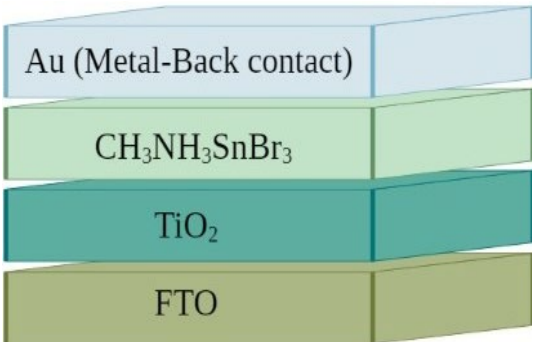

Fig. 1 Schematic structure of the device.

Table 1.Simulation parameters [14,15].

Parameter	FTO	TiO_2	$CH_3NH_3SnBr_3$
Thickness(μm)	0.4	0.05	0.5
E_g (eV)	3.5	3.26	1.3
χ(eV)	4.0	4.2	4.17
ε_r	9.0	10.0	10.0
N_C(cm^{-3})	1.8×10^{18}	1.8×10^{18}	1.8×10^{18}
N_V(cm^{-3})	2.2×10^{18}	2.2×10^{18}	2.2×10^{18}
μ_n(cm^2/Vs)	20	20	1.6
μ_p(cm^2/Vs)	10	10	1.6
N_D(cm^{-3})	1×10^{19}	1×10^{17}	0
N_A(cm^{-3})	0	0	1×10^{13}

Table 2. Interface parameter $TiO_2/CH_3NH_3SnBr_3$ [14,15].

Parameter	$TiO_2/CH_3NH_3SnBr_3$
Defect type	Neutral
$\sigma_n(cm^{-2})$	1×10^{-15}
$\sigma_p\ (cm^{-2})$	1×10^{-15}
Energy distribution	Single
Energy level with respect to E_V (above eV) (eV)	.600
Characteristic energy(eV)	-
$N_t(cm^{-3})$	1×10^{10}

Table 3. Initial values of cell performance parameters.

V_{OC}(v)	.6461
$J_{SC}\ (mA/cm^2)$	28.810590
FF (%)	67.86
η(%)	12.63

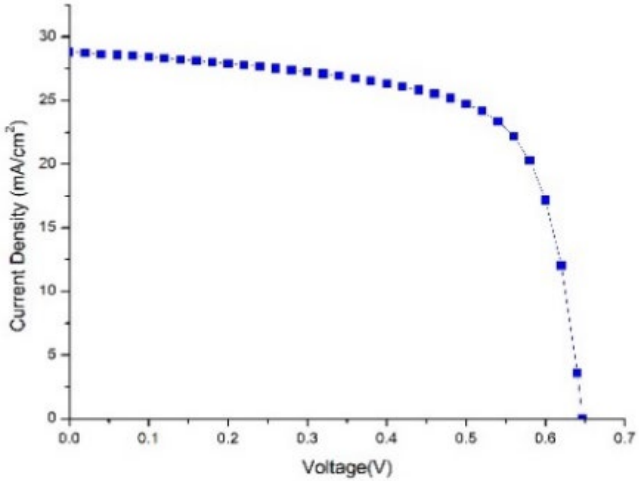

Fig. 2. Current density-Voltage curve.

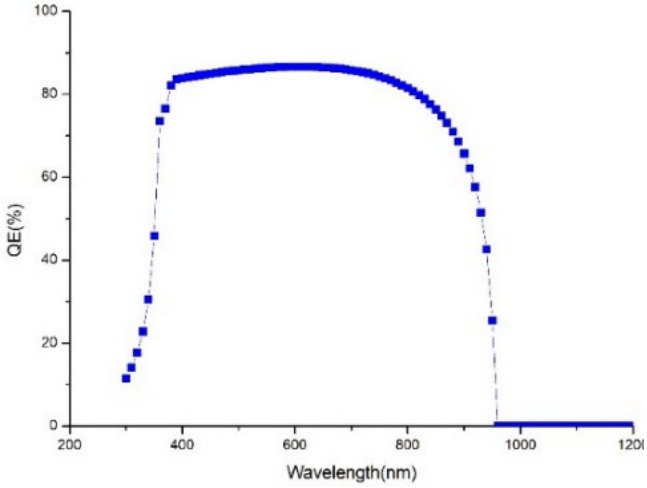

Fig. 3. Quantum efficiency-waelength curve.

3. Results and discussion

3.1. Effect of changing defect density (N_t) and absorber thickness

The defect density of the absorber layer is varied from 1×10^{14} to 1×10^{19} cm^{-3}. The corresponding diffusion length is calculated and tabulated in Table 4 using the equation

$$L = \sqrt{(D \times \tau)},$$ where D is the diffusion coefficient

$$D = \frac{KT}{q}\mu$$, where μ is the mobility of charge carriers

and

$$\tau = \frac{1}{\sigma x N_t x V_{th}}$$

σ is the capture cross-section of electrons and holes, N_t is the defect density and $V_{th}$is the thermal velocity of electrons and holes.

On increasing the defect density, the lifetime of the carrier decreases and diffusion length decreases and causes more recombination. The efficiency graph is plotted in Fig. 4 according to the variation of absorber thickness for different values of diffusion length. The optimum defect density is chosen as $10^{14}cm^{-3}$ as it provides better efficiency and the corresponding diffusion length is 2.034μm. The efficiency reaches 13.24% at this value. The optimum thickness is chosen as 1μm considering the practical implementation and optimum diffusion length.

Table 4. Variation of diffusion length with defect density.

$N_t(cm^{-3})$	10^{14}	10^{15}	10^{16}	10^{17}	10^{18}	10^{19}
L(μm)	2.034	.643	.203	.064	.0203	.00643

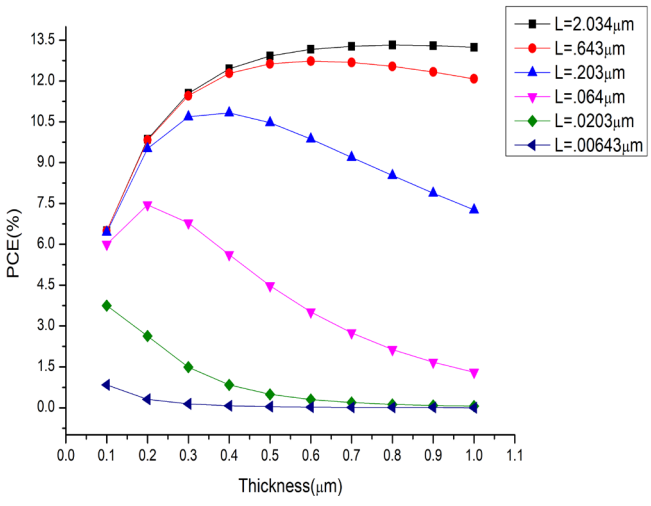

Fig. 4. Variation of power efficiency with absorber thickness at different diffusion lengths of the absorber layer.

3.2. Effect of changing the doping concentration of the absorber layer

The doping concentration of the absorber layer is varied from 10^{14} cm^{-3} to 10^{18} cm^{-3} and Fig. 5 shows the variation of V_{oc}, J_{sc}, FF, PCE with doping concentration. V_{oc} shows a sudden increase to 0.7955V at 10^{16} cm^{-3} and we get a maximum value of 15.96% efficiency at this doping

concentration. Hence we select 10^{16} cm^{-3} as the optimum value in the present work. The decrease in efficiency after this point is due to the increase in Auger recombination with high doping [17].

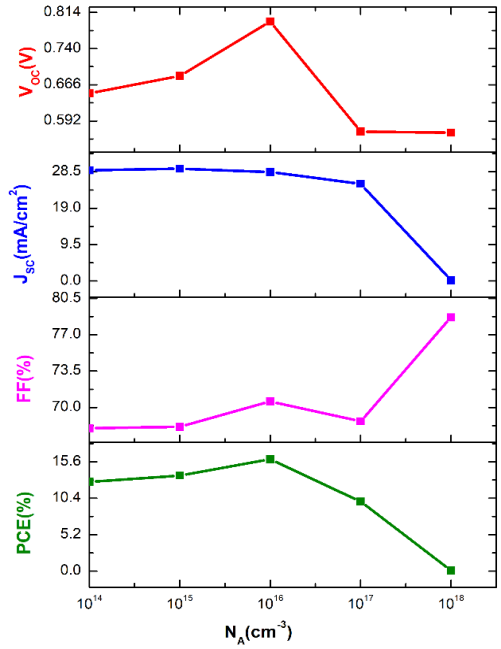

Fig. 5. Variation of cell performance parameters with doping concentration of absorber layer.

3.3. Effect of ETL thickness and doping concentration

The ETL thickness is varied from .01µm to .07 µm and the variation of cell performance parameters is depicted in Fig. 6. It is evident in Figure 6 that the efficiency of the solar cell increases up to 13.85% on decreasing the thickness of the ETL to 0.01µm and considering the practical implementation of an efficient solar cell, we select .02µm as the optimum value of ETL thickness.

The doping concentration is varied from 10^{16} to 10^{20} cm^{-3} and the variation graph is plotted in Fig. 7, where the efficiency increases with an increase in the doping concentration of the ETL. The efficiency reaches 15.79% at 10^{20} cm^{-3}. While considering the manufacturing difficulty, we have chosen 10^{18} as the optimum value.

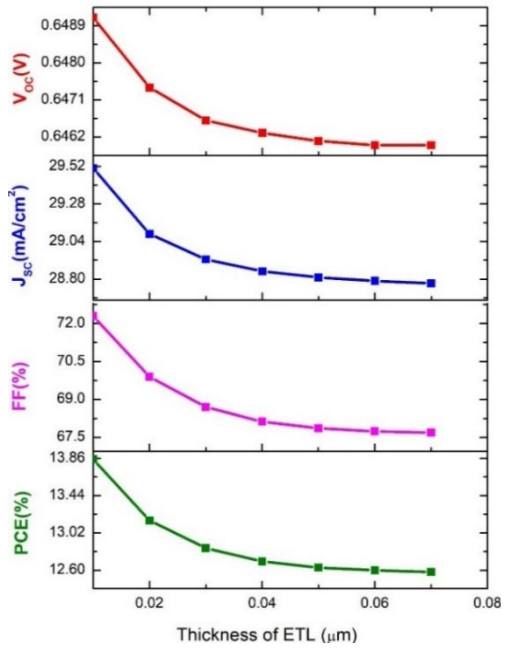

Fig. 6. Effect of ETL thickness on cell performance parametrs.

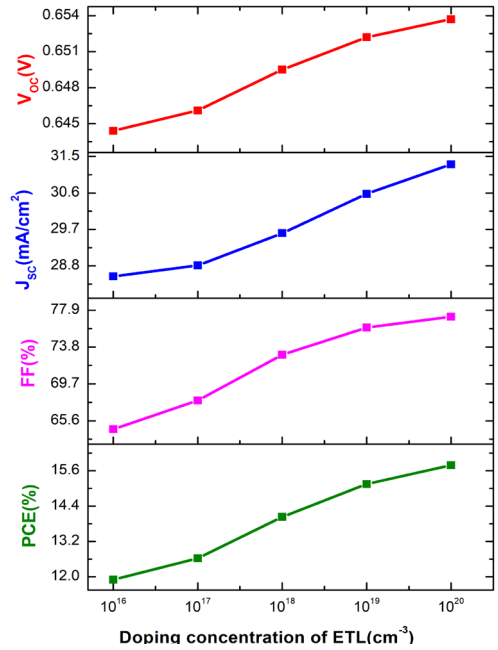

Fig. 7. Effect of ETL doping concentration on cell performance parameters.

3.4. Effect of operating temperature

The temperature is kept at 300K in the initial simulation and we have varied the temperature from 300K to 400K in order to find the influence of temperature in V_{oc}, J_{sc}, FF, and PCE.The variation graph is plotted in Fig. 8. It is found that V_{oc}, J_{sc}, FF, and PCE of the cell decreases on increasing the temperature. The efficiency of the cell decreases to 9.21% at 400K. An increase in the temperature causes an increase in the interfacial defects. So the diffusion length decreases and causes a reduction in the efficiency of the cell. The recombination rate of the charge carriers also increases with temperature which causes the reduction in efficiency[18] . Hence 300 K has been set as the optimum temperature.

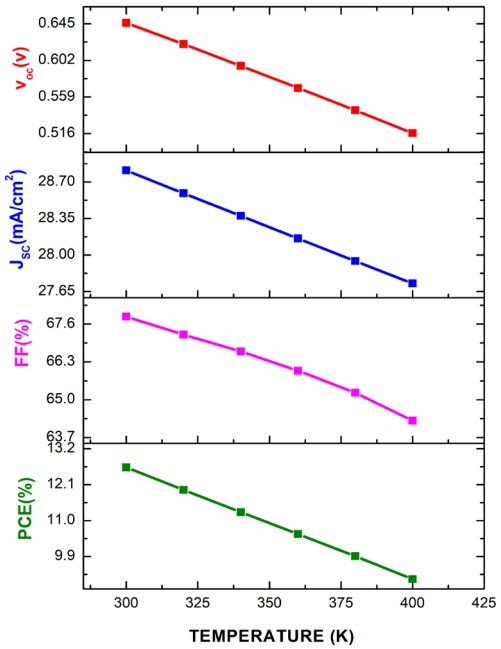

Fig. 8. Effect of operating temperature on cell performance parameters.

3.5. Effect of metal work function

Simulation of the structure is repeated with different back metal contacts such as Au, Cu doped C, Ag, Pt, Cu and Fe. Table 5 shows the work function of these metals.The variation of performance parameters with work function is plotted in Fig. 9. It is seen that as the work function increases the efficiency increases. This is because the barrier height of the majority charge carriers decreases with increase in the work function of the metal[14,19]. Since Pt is expensive,Au is selected as the back contact metal in this work.

Table 5. Metal work function for different materials.

Back metal contact	Au	Cu dopped C	Ag	Pt	Cu	Fe
Metalwork function(eV)	5.1	5.0	4.74	5.7	4.6	4.8

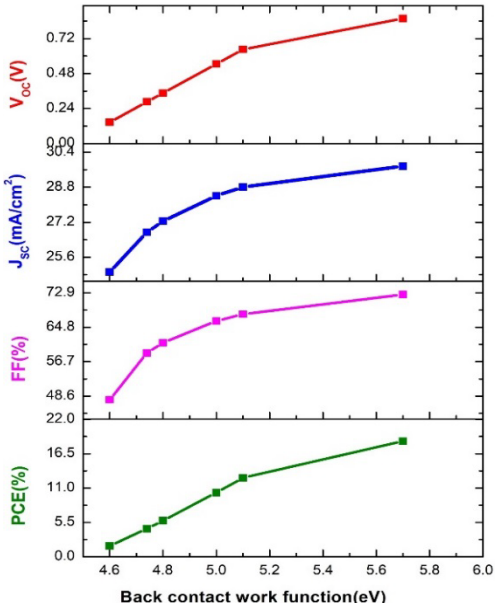

Fig. 9. Effect of back metal contact on cell performance parameters.

3.6. Effect of interface defect density

The influence of the $TiO_2/CH_3NH_3SnBr_3$ interface defect density is studied in this work. The defect density of the interface is varied from10^{10} to $10^{15}cm^{-3}$ keeping other parameters constant. It is noted that the value of V_{oc} and PCE remains almost constant up to $10^{11}cm^{-3}$ and starts decreasing from 10^{11} to 10^{13} and again remains constant up to $10^{15}cm^{-3}$at a lower value. The efficiency of the perovskite solar cell decreases with an increase in the defect density due to the increase in recombination rate. An efficiency of 16.36% and 12.64% is obtained for $10^{10}cm^3$ and $10^{15}cm^{-3}$. Fig.10 illustrates this and hence we selected $10^{10}cm^{-3}$ as the optimum value.

The optimized value of each parameter is shown in Table 6. The simulation is repeated with all these optimised values and the performance parameters obtained are shown in Table 7. Fig. 11 depicts the variation of the Voltage-Current density curve for initial values, for each optimized parameter and for all optimized parameters.

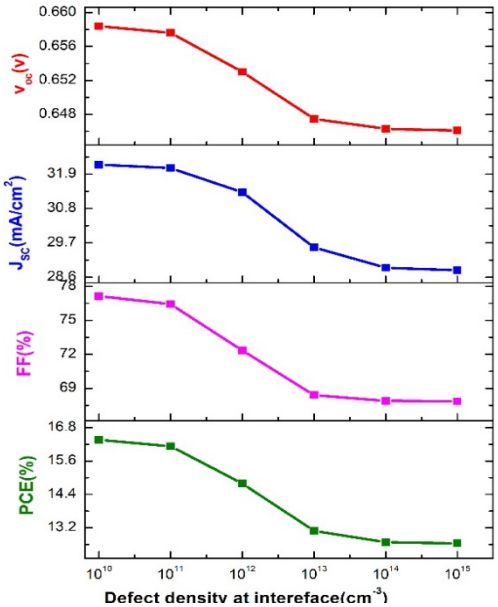

Fig. 10. Effect of interface defect density on cell performance parameters.

Table 6. Optimized parameters.

Thickness of absorber	N_t	NA	Thickness of ETL	N_D	Temperature	Back Contact	Interface N_t
1 µm	10^{14}cm^{-3}	10^{16} cm^{-3}	.02µm	10^{18} cm^{-3}	300K	Au	10^{10}cm^{-3}

Table 7. Device performance parameters after optimization.

V_{oc} (v)	.8897
J_{sc} (mA/cm^2)	32.900726
FF (%)	42.11
η(%)	24.02

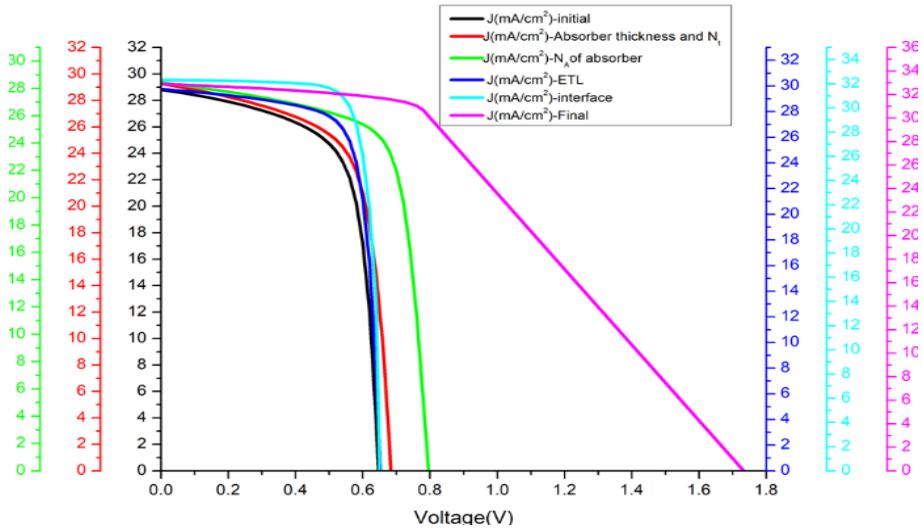

Fig. 11. Current density –voltage characteristics of initial optimization, optimum values of each parameter and final optimization.

4. Conclusions

Demand for renewable energy sources is increasing nowadays due to the increase in the population. Hence we are forced to use clean energy technologies to meet the the increasing energy demand. Solar energy is the most abundant energy. In this work, we simulated an HTL-free perovskite solar cell with $CH_3NH_3SnBr_3$ as the absorber layer and TiO_2 as the ETL layer using the software SCAPS 1-D and studied the variation in cell performance parameters on changing certain parameters like thickness, defect density and doping concentration of absorber, thickness and doping concentration of ETL, temperature and defect density of the absorber/ETL interface. The final simulation was carried out by the selected values. The maximum impact on efficiency is obtained by varying the doping concentration of the absorber and ETL. By using the optimized values we have reached a maximum efficiency of 24.02% from an initial efficiency of 12.63%. This work proposes guidelines for the fabrication of a simple, HTL-free, efficient, non-toxic perovskite solar cell.

References

[1] Sunny, Adil et al., AIP Advances 11.6 (2021); https://doi.org/10.1063/5.0049646
[2] Ouslimane, Touria et al., Heliyon 7.3 (2021); https://doi.org/10.1016/j.heliyon.2021.e06379
[3] Haider, Syed Zulqarnain, Hafeez Anwar, Mingqing Wang, Semiconductor Science and Technology 33.3 (2018): 035001; https://doi.org/10.1088/1361-6641/aaa596
[4] Lin, Lingyan et al., Materials Science in Semiconductor Processing 90 (2019): 1-6; https://doi.org/10.1016/j.mssp.2018.10.003
[5] Fatema, Kanij, and Md Shamsul Arefin, Optical Materials 125 (2022): 112036; https://doi.org/10.1016/j.optmat.2022.112036
[6] Serrano-Lujan, Lucia et al., Advanced Energy Materials 5.20 (2015): 1501119; https://doi.org/10.1002/aenm.201501119
[7] Hao Feng et al., Nature photonics 8.6 (2014): 489-494; https://doi.org/10.1038/nphoton.2014.82
[8] Sani Faruk et al., Materials 11.6 (2018): 1008; https://doi.org/10.3390/ma11061008
[9] Anwar, Farhana et al., International Journal of Photoenergy 2017 (2017); https://doi.org/10.1155/2017/9846310
[10] Zhao, Xin-Gang et al., Journal of the American Chemical Society 139.7 (2017): 2630-2638; https://doi.org/10.1021/jacs.6b09645
[11] Abdelaziz, Saied et al., Optical Materials 101 (2020): 109738; https://doi.org/10.1016/j.optmat.2020.109738
[12] Hao, Liangsheng et al., Optical and Quantum Electronics 53 (2021): 1-17; https://doi.org/10.1007/s11082-021-03175-5
[13] Lang, Li et al., Physics Letters A 378.3 (2014): 290-293; https://doi.org/10.1016/j.physleta.2013.11.018
[14] Samiul Islam Md et al., Nanomaterials 11.5 (2021): 1218; https://doi.org/10.3390/nano11051218
[15]Patel Piyush K., Scientific reports 11.1 (2021): 3082; https://doi.org/10.1038/s41598-021-82817-w
[16] Thomas Titu, Renewable Energy Research and Applications 4.2 (2023): 159-169.
[17] Bag, Atanu et al., Solar Energy 196 (2020): 177-182; https://doi.org/10.1016/j.solener.2019.12.014
[18] Alam, Intekhab, Md Ali Ashraf, Energy Sources, Part A: Recovery, Utilization, and Environmental Effects (2020): 1-17; https://doi.org/10.1080/15567036.2020.1820628
[19] Shamna, M. S., K. S. Nithya, K. S. Sudheer, Materials Today: Proceedings 33 (2020): 1246-1251; https://doi.org/10.1016/j.matpr.2020.03.488